# Chain-End Structures in Polypropylene Prepared with δ-$TiCl_3$/$Et_2AlCl$ Catalytic System in the Presence of Hydrogen

**Tetsuo Hayashi,* Yoshio Inoue, and Riichirô Chûjô**

*Department of Polymer Chemistry, Tokyo Institute of Technology, 2-12-1, O-okayama, Meguro-ku, Tokyo 152, Japan*

**Tetsuo Asakura**

*Department of Polymer Engineering, Faculty of Technology, Tokyo University of Agriculture and Technology, Koganei, Tokyo 184, Japan.* *Received December 23, 1987*

ABSTRACT: The chain-end structures were studied on the basis of $^{13}C$ NMR and INEPT (insensitive nuclei enhanced by polarization transfer) spectra for polypropylene (PP) polymerized with δ-$TiCl_3$/$Et_2AlCl$ catalytic system in the presence of molecular hydrogen. The chain-end structure I

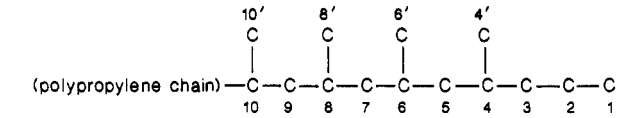


I

was identified by referring to the chemical shift data for the model compounds. The mechanism of the initiation reaction proposed by Natta was first supported by NMR measurements, because the structure (I) could be produced with the initiation reaction by the primary insertion of propylene on the metal–hydrogen bond and the subsequent propylene propagation reactions. The chain-end structures produced by the termination reactions with hydrogen were also identified. The split peaks of the carbons in the chain end groups, which arise from the different stereosequences in the chain end, were observed in the spectrum of the fraction of PP soluble in boiling heptane. The assignments of the split peaks were provided on the basis of the chemical shift calculation using the γ-effect on $^{13}C$ chemical shift and the Mark's rotational isomeric state model. The tetrad tacticities reflecting the configurational relationships among the methine carbons 4, 6, 8, and 10 were examined in detail from the split peaks of carbon 3 in structure I. From the analysis of the polymerization mechanism based on the two-site model, it is demonstrated that the steric controls of the initiation reaction at the asymmetric and symmetric sites are as strong as those of the isotactic and atactic propagation reactions, respectively.

## Introduction

On the basis of $^{13}C$ NMR spectra, Zambelli et al.[1-4] have studied chain-end structures in polypropylene (PP), which have thrown light on the initiation and the termination reactions of propylene polymerization. In recent years, by improvements of the sensitivity and the resolution of $^{13}C$ NMR spectra, $^{13}C$ NMR has become the most powerful method to investigate the chain-end structures of polypropylene.

By referring to the observed $^{13}C$ chemical shifts of the model compounds for polypropylene,[1] Zambelli et al.[2] have identified the chain-end structures in $^{13}C$-enriched polypropylene polymerized with various catalytic systems. The chain-end structures produced with the initiation reactions by the primary and secondary insertions of propylene on the metal–carbon bond have been also identified by them.[2] From the $^{13}C$ NMR spectrum of the isotactic polypropylene polymerized with δ-$TiCl_3$/$Al(CH_3)_3$/$Zn(CH_3)_2$ catalytic systems, they[2] demonstrated that both the initiation and propagation reactions proceed through primary insertion of the monomer on the transition metal–carbon bond in the stereoregular type titanium based catalytic system. Further, Zambelli et al.[3,4] have investigated the formation process of the initiation species, the mechanisms of the monomer insertion on the metal–carbon bond, and the steric control by chiral catalytic centers from the $^{13}C$ NMR spectra of selectively $^{13}C$-enriched end groups of polypropylene.

The chain-end structures in ethylene–propylene copolymers have been studied on the basis of $^{13}C$ NMR spectra.[5,6] Lately, Cheng[6] summarized the possible schemes for the initiation, chain transfer, and termination reactions with the comprehensive data of $^{13}C$ NMR chemical shifts of the carbons in the various chain-end structures.

The propagation mechanism of polypropylene has been examined in detail by using the values of tactic *n*-ad configurations determined by $^{13}C$ NMR spectra. It is concluded that neither Bernoullian nor low-order Markovian models describe the propagation mechanism of propylene.[7-10] The two-site model proposed by Chûjô[7] and Zambelli et al.[8] is adequate to describe the propagation mechanism. According to this model, the polymer was considered to be the mixture of the products from two independent processes. At one site, the propylene propagation proceeds under control of a symmetric Bernoullian model (selection between meso and racemo), and at the other site the propagation mechanism obeys an asymmetric Bernoullian model (selection between dextro and levo). The analytical results for the polypropylene samples polymerized with various Ziegler–Natta catalytic systems based on the two-site model have suggested that the asymmetric model corresponds to a site producing a highly isotactic polypropylene and the symmetric model to a site producing an atactic polypropylene.[8-11] Thus, it is expected that the chain-end structures produced by the initiation and termination reactions should reflect the respective steric controls at two different sites.

In this paper, we will analyze the chain-end structures of polypropylene (PP) polymerized with the δ-$TiCl_3$/$Et_2AlCl$ catalytic system in the presence of molecular hydrogen. When hydrogen is present in the polymerization, it induces the termination reaction producing metal hydride which regenerates the active center (metal–carbon

0024-9297/88/2221-2675$01.50/0 

bond) by the primary insertion of propylene on the metal–hydrogen bond.[12] The chain-end structure produced by this initiation reaction is predicted as follows:

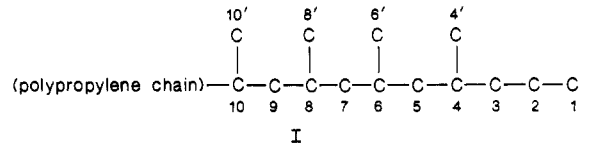


I

From the $^{13}C$ NMR spectra of PP and the fraction (PPS7) of PP soluble in boiling heptane, the structure I will be identified by referring to the chemical shifts of the carbons in the model compounds of polypropylene observed by Zambelli et al.[1] The resonance of carbon 3 in structure I is expected to show the split peaks reflecting the different relationships among the configurations of the methine carbons 4, 6, 8, and 10 (structure I). The assignments of these split peaks can be provided on the basis of the chemical shift calculation using the $\gamma$-effect[13,14] on $^{13}C$ chemical shifts and Mark's rotational isomeric state model.[15] The chain-end structures produced with the termination reaction by molecular hydrogen will be discriminated from those produced by the other possible initiation reactions. The $^1H$-decoupled INEPT (insensitive nuclei enhanced by polarization transfer) method[16,17] with the delay time ($\Delta$) of $3/4J$ ($J$ is the coupling constant between $^{13}C$ and $^1H$) prior to data acquisition, which distinguishes the methylene peaks from the methine and methyl peaks, will be used to remove the ambiguities in the assignments of the peaks of the carbons included in the end groups of the different chain-end structures. The ambiguity will be removed by the difference of the sign of INEPT signals among the methylene and the other carbons. Thus, this method is very effective when the chemical shifts of methylene and methyl or methine peaks are close to each other. Further, the tacticities in the chain-end structures (I) will be determined from the relative areas of the split peaks of carbon 3 in structure I. On the basis of the two-site model, the respective steric controls of the initiation reaction at two different sites will be compared with those of the propagation reaction by using the values of the tacticities in structure I and those in the polypropylene chain.

## Experimental Section

**Material.** Highly isotactic polypropylene polymerized with the Ziegler–Natta catalytic system $\delta$-$TiCl_3$/$Et_2AlCl$, which is known to produce highly stereoregular polymers, was presented by Tokuyama Soda Co., Ltd. The weight-average ($\bar{M}_w$) and number-average ($\bar{M}_n$) molecular weights are 30 2000 and 37 700, respectively. Hereafter this sample will be abbreviated as PP. The other sample, PPS7, is the fraction of PP soluble in boiling heptane, and its $\bar{M}_w$ and $\bar{M}_n$ are 2500 and 1000, respectively. The values of $\bar{M}_w$ and $\bar{M}_n$ were determined by gel permeation chromatography. The weight fraction of PPS7 in the whole polymer is 0.035.

**NMR Measurements.** $^{13}C$ NMR spectra were recorded at 120 °C on a JEOL GSX-270 spectrometer at 67.8 MHz. The sample solutions, in a 10-mm o.d. glass tube, were prepared in *o*-dichlorobenzene (90 vol %)/benzene-$d_6$ (10 vol %) to give 0.1 g(polymer)/cm$^3$(solvent). Benzene-$d_6$ provided the signal for the $^2H$ NMR internal lock. In all measurements broad-band noise decoupling was used to remove $^{13}C$–$^1H$ couplings, the pulse angle was 90°, the pulse repetition time was 15 s, and the free induction decays (FID) were stored in 32K data points by using a spectral window of 10000 Hz. The number of accumulated FIDs was 8000. Hexamethyldisiloxane was used as an internal reference (2.03 ppm downfield from the resonance of tetramethylsilane). For the quantitative measurements, the pulse repetition time was set to be 25 s, which was more than 5 times the spin–lattice relaxation times of the most mobile methyl carbons at the chain end (4.0–4.8 s[6]). The $^1H$-decoupled INEPT[16,17] method, in which the delay time ($\Delta$) prior to data acquisition is equal to $3/4J$ (where $J$ is the $^1H$–$^{13}C$ spin–spin coupling constant), was used to distinguish methylene peaks from methine or methyl peaks.

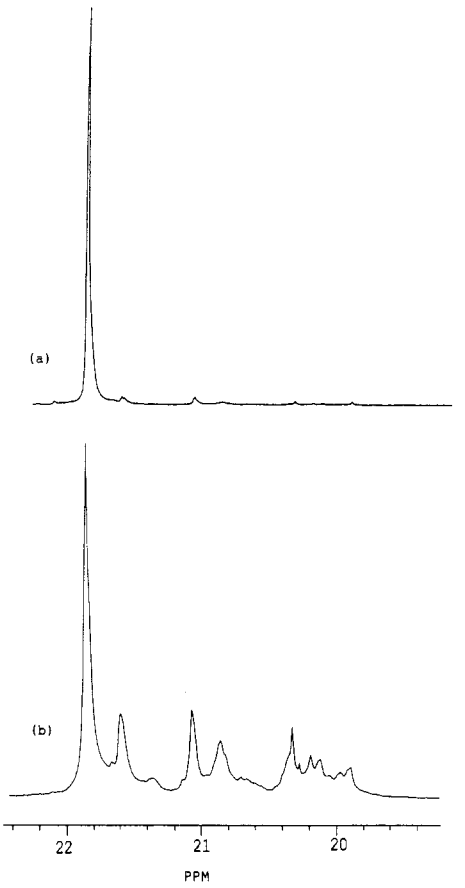


**Figure 1.** Methyl resonance region of the $^{13}C$ NMR spectra of (a) polypropylene (PP) and (b) the fraction (PPS7) of PP soluble in boiling heptane.

**$^{13}C$ NMR Chemical Shift Calculation.** $^{13}C$ NMR chemical shifts of the chain-end carbons in PP and PPS7 were predicted by the calculation using the Mark's RIS model[8] of ethylene–propylene copolymer and the $\gamma$-effect on $^{13}C$ NMR chemical shift. In Mark's RIS model, the values of the statistical weights, $\eta$, were taken to be 1.0, and $\omega$ and $\tau$ were characterized with $E_\omega$ = 8400 J mol$^{-1}$ and $E_\tau$ = 2100 J mol$^{-1}$. The value of the $\gamma$-effect was taken to be −5.3 or −3.7 ppm upfield relative to those of the trans arrangement, depending on the species of carbon atom in the calculation for polypropylene as proposed by Tonelli.[13,14] In the case of chain-end structure, the value of −3.7 ppm was assumed as the $\gamma$-effect of methyl and methylene carbons on the $^{13}C$ chemical shift of methylene carbon. The calculation was performed at 120 and 140 °C, corresponding with the experimental conditions.

## Results and Discussion

**Analyses of the Chain-End Structures.** In parts a and b of Figure 1 are shown the methyl resonance regions of the $^{13}C$ NMR spectra of the highly isotactic polypropylene (PP) and the fraction (PPS7) of PP soluble in boiling heptane, respectively. These spectra indicate that the tacticities of PP and PPS7 are mainly isotactic. The fractions of meso diad in PP and PPS7 are 0.941 and 0.632, respectively, according to our previous methyl-heptad configurational analysis.[11]

In parts a and b of Figure 2 are shown the chain-end methyl resonance regions of the $^{13}C$ NMR spectra of PP and PPS7. The split peaks are observed at 14.49 and 14.44 ppm in both spectra. The peaks at 14.12, 13.95, and 11.12 ppm are observed only in the spectrum of PPS7. In Table

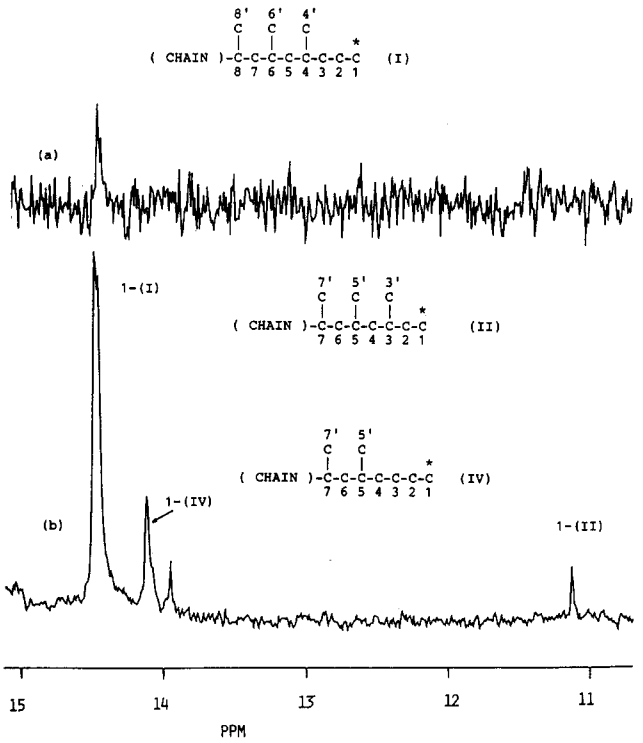


**Figure 2.** Chain-end methyl resonance regions of the $^{13}C$ NMR spectra of (a) PP and (b) PPS7.

**Table I**
**Chemical Shifts of 2,4,6-Trimethylnonane (A) and 2,4,6-Trimethyloctane (B) Observed by Zambelli et al.[1] at 140 °C**

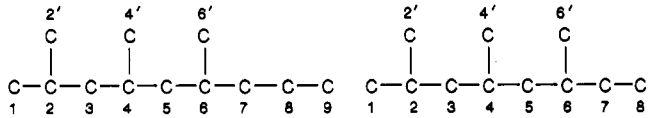


| carbon | chem shift[a] compound A racemo (4R,6R) | compound A meso (4R,6S) | compound B racemo (4R,6R) | compound B meso (4R,6S) |
|---|---|---|---|---|
| 1 | 23.56 | 23.77 | 23.54 | 23.74 |
| 2 | 26.07 | 26.07 | 26.01 | 26.01 |
| 2′ | 22.90 | 22.74 | 22.89 | 22.77 |
| 3 | 48.60 | 48.03 | 48.50 | 47.96 |
| 4 | 29.02 | 29.15 | 28.96 | 29.07 |
| 4′ | 20.44 | 21.08 | 20.43 | 20.98 |
| 5 | 46.23 | 46.59 | 45.66 | 45.96 |
| 6 | 30.78 | 30.82 | 32.55 | 32.61 |
| 6′ | 20.12 | 20.74 | 19.56 | 20.16 |
| 7 | 40.92 | 40.19 | 30.80 | 29.95 |
| 8 | 20.48 | 20.36 | 11.30 | 11.16 |
| 9 | 14.40 | 14.40 | | |

[a] Chemical shifts are expressed in ppm from the resonance of tetramethylsilane.

I are shown the chemical shifts of the carbons in 2,4,6-trimethylnonane (A) and 2,4,6-trimethyloctane (B) as model compounds of polypropylene, which have been observed at 140 °C by Zambelli et al.[1] The assignments of the peaks at 14.49, 14.44, and 11.12 ppm are provided by referring to the chemical shifts shown in Table I. The chemical shifts of carbon 8 (8-(B)) in compound B and the carbon 9 (9-(A)) in compound A correspond well with the observed peaks at 11.12 and 14.49 ppm, respectively. The peaks at 14.49 and 14.44 ppm are therefore assigned to carbon 1 in the chain-end structure I in a polypropylene chain, which is similar to the structure of compound A.

**Table II**
**Chemical Shifts ($\nu$) of Carbon 9 in Model Compound A and Carbon 8 in Model Compound B**

| compd | carbon | $\nu_{obsd}$, ppm | $\Delta\nu_{obsd}$,[a] ppm | calcd $\gamma$-effect, ppm | $\Delta\nu_{calcd}$,[a] ppm |
|---|---|---|---|---|---|
| A, meso | 9 | 14.40 | 0.0 | −1.623 | 0.0 |
| A, racemo | 9 | 14.40 | 0.0 | −1.654 | −0.031 |
| B, meso | 8 | 11.16 | −0.14 | −6.570 | −0.031 |
| B, racemo | 8 | 11.30 | 0.0 | −6.539 | 0.0 |

[a] Chemical shifts are expressed relative to the peak appearing at the lowest field, which is set to 0.00 ppm.

The peak at 11.12 ppm is assigned to carbon 1 in structure II as follows:

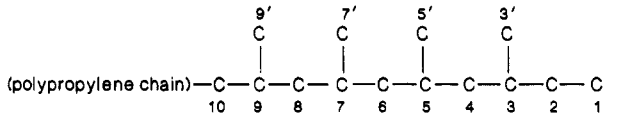


II

However, the assignments of the split peaks at 14.49 and 14.44 ppm are not provided from the chemical shift of carbon 9-(A), which does not show the stereosequence dependence of $^{13}C$ chemical shift due to the difference in the structure of the model compound (A) with meso and racemo configurations. The chemical shift calculation using the $\gamma$-effect on $^{13}C$ NMR chemical shift[13,14] and Mark's RIS model[15] can well predict the stereosequence dependence of the $^{13}C$ chemical shift.[18] The chemical shift change due to the $\gamma$-effect was calculated for carbons 8-(B) and 9-(A) and the results are shown in Table II with the observed ones. The calculated results indicate that the respective chemical shift differences in carbon 9-(A) and carbon 8-(B) are 0.031 ppm, which arise from the different diad configurations around the methylene carbon 5 in compounds A and B, respectively. The chemical shift of carbon 8 in the racemo form of compound B is predicted to be 0.031 ppm larger than that in the meso form of compound B. Thus, the relative positions of the peaks of carbon 8-(B) are predicted reasonably by the $\gamma$-effect calculation. Similarly, the peak of carbon 9 in the meso form of compound A is predicted to appear at lower field compared with that in the racemo form. From the calculated results shown in Table II, the peaks at 11.12 ppm is assigned to carbon 1 (1-(II)) in structure II with the meso diad configuration around the methylene carbon 4, because the observed chemical shift of 11.12 ppm coincides with that of carbon 8 in the meso form of compound B. The peaks at 14.49 and 14.45 ppm are assigned to carbon 1 (1-(I)) in structure I with the respective meso and racemo diad configurations around methylene carbon 5. Here, we will define the nomenclature of the tactic structures at the chain end in order to simplify the description of these stereosequence-dependent structures. As shown in Figure 3, the symbols "ME", "ET", "PR", and "BU" correspond to the kinds of *n*-alkyl end groups, i.e., methyl, ethyl, propyl, and butyl, respectively, in the chain-end structures, and the diad configurations around the methylene carbons of interest are expressed by meso (*m*) and racemo (*r*). For example, when the end group is propyl and methine carbons 4 and 6 have attached methyl substituents 4′ and 6′ with meso diad configuration around methylene carbon 5, the tacticity at the chain-end is denoted as PR-meso. If the tacticity at the chain-end structure depends on the longer sequences than that of diad, the tacticity is named XY-*n*-ad according to our nomenclature, where XY represents the name of *n*-alkyl group and *n*-ad corresponds to triad, tetrad, and so on. Using this nomenclature, the

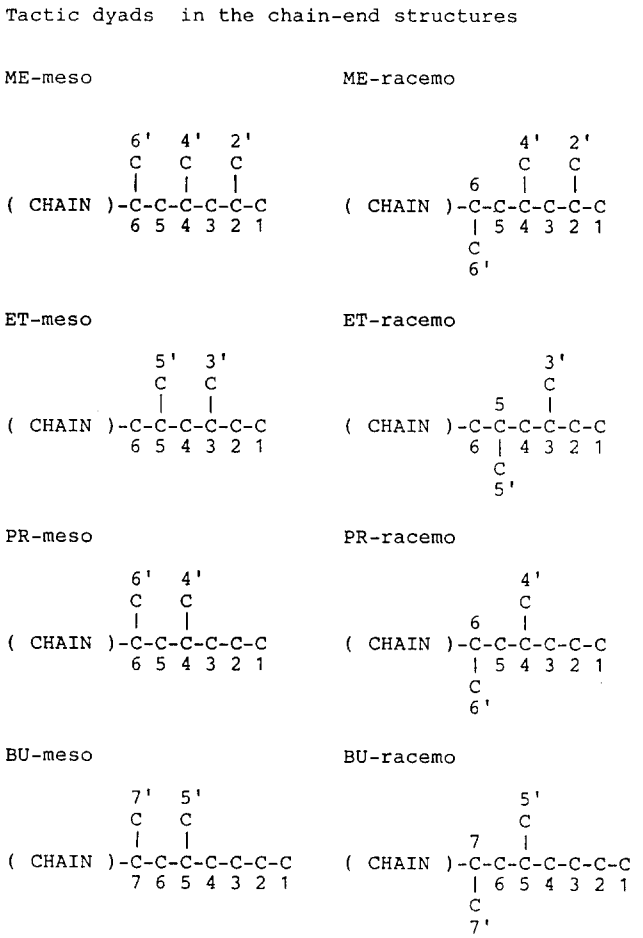


**Figure 3.** Nomenclature of the tactic structures at the chain end.

**Table III**
**Chemical Shifts of Methyl Carbons 1 in Chain-End Structures I and II**

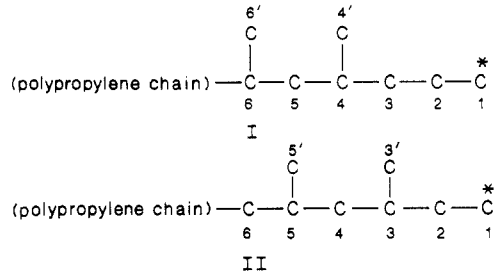


| chem shift, whole polym, ppm | chem shift, PPS7, ppm | carbon | diad in chain end-tacticity[a] |
|---|---|---|---|
| | 11.12 | 1-(II) | ET-meso |
| 14.45 | 14.44 | 1-(I) | PR-racemo |
| 14.49 | 14.49 | 1-(I) | PR-meso |

[a] The nomenclature of the tactic structure is shown in Figure 3.

peak at 11.12 ppm assigned to carbon 1 in structure II is expressed as ET-meso, as shown in Table III. In a similar way, the peaks at 14.49 and 14.44 ppm are assigned to carbon 1 in structure I of PR-meso and PR-racemo, respectively. The assignment of the peak at 14.12 ppm will be described later in this paper. The peak at 13.95 ppm is still unidentified.

In parts a and b of Figure 4 are shown the regions from 39 to 41 ppm in the spectra of PP and PPS7. The peak at 39.8 ppm is observed in both spectra. A number of split peaks are observed in the spectrum of PPS7. The observed[1] and calculated chemical shifts of carbon 7 (7-(A))

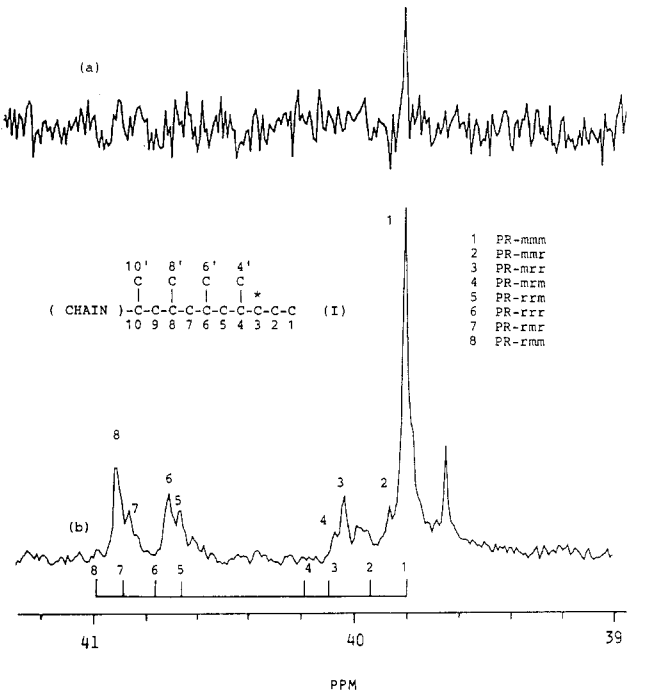


**Figure 4.** $^{13}C$ NMR spectra of methylene carbon 3 in the chain-end structure I of (a) PP and (b) PPS7. The predicted shifts are shown as the stick spectrum at the bottom of this figure.

**Table IV**
**Observed and Calculated Chemical Shifts ($\nu$) of Methylene Carbon 7 in Model Compound A**

| form | $\nu_{obsd}$,[a] ppm | $\Delta\nu_{obsd}$,[b] ppm | calcd $\gamma$-effect, ppm | $\Delta\nu_{calcd}$,[b] ppm |
|---|---|---|---|---|
| meso (4*R*,6*S*) | 40.19 | −0.73 | −1.908 | −0.796 |
| racemo (4*R*,6*R*) | 40.92 | 0.0 | −1.112 | 0.0 |

[a] Cited from ref 1. [b] Chemical shifts are expressed relative to the peak appearing at the lowest field which is set to 0.00 ppm.

in the meso and racemo forms of compound A are shown in Table IV. The chemical shift difference between the resonances of the stereochemically different carbons 7-(A), is reasonably predicted by calculation via the $\gamma$-effect. By referring to the results for carbon 7-(A), the observed peaks in Figure 4 are assigned to carbon 3 (3-(I)) in structure I. However, the assignments of a number of split peaks observed in the spectrum of PPS7 by referring to the chemical shifts of carbon 7-(A) are impossible owing to insufficient chain length of model compound A, because it is expected that the chemical shift of carbon 3-(I) is affected by a configurational sequence longer than a diad tactic sequence. The chemical shifts calculation via the $\gamma$-effect was therefore performed on carbon 3 in the chain-end structure I of the tactic tetrads (PR-tetrads), which depends on the configurational relationships among the methine carbons 4, 6, 8, and 10. The polypropylene chain in structure I is simplified to be composed of 20 meso-diad sequences followed by the chain-end $C_{10}$–$C_1$ carbons of structure I, because PPS7 is mainly isotactic. The calculated results are shown in Table V. The peak observed at 39.80 ppm is assigned to carbon 3-(I) of the PR-*mmm* tetrad, because the intensity of this peak is nearly equal to that of the peak at 14.49 ppm and the PR-*mmm* peak of carbon 3-(I) is predicted by the calculation to appear at the highest field, as illustrated by a stick spectrum in Figure 4b. By comparison between the observed and calculated spectra, the assignments of the split peaks numbered 1–8 are provided as shown in Table V. Two peaks appearing at 39.63 and 39.98 ppm are unidentified

**Table V**
**Calculated and Observed Chemical Shift Differences ($\Delta\nu$) of Carbon 3 in the Chain-End Structure I and Observed Chemical Shifts ($\nu$) in the Spectrum of PPS7**

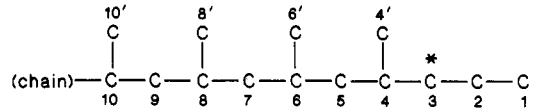


I

| tetrad in the chain end | calcd | | obsd (PPS7)[b] | | |
|---|---|---|---|---|---|
| | $\gamma$-effect, ppm | $\Delta\nu_{calcd}$,[a] ppm | peak | $\nu_{obsd}$, ppm | $\Delta\nu_{obsd}$,[a] ppm |
| PR-*mmm* | −2.132 | 0.0 | 1 | 39.80 | 0.0 |
| PR-*mmr* | −1.991 | 0.141 | 2 | 39.86 | 0.06 |
| PR-*mrr* | −1.833 | 0.299 | 3 | 40.03 | 0.23 |
| PR-*mrm* | −1.732 | 0.400 | 4 | 40.07 | 0.27 |
| PR-*rrm* | −1.260 | 0.872 | 5 | 40.66 | 0.86 |
| PR-*rrr* | −1.174 | 0.958 | 6 | 40.71 | 0.91 |
| PR-*rmr* | −1.047 | 1.085 | 7 | 40.86 | 1.06 |
| PR-*rmm* | −0.941 | 1.191 | 8 | 40.91 | 1.11 |

[a] Chemical shifts are expressed relative to the peak appearing at the lowest field which is set to 0.00 ppm. [b] Corresponding spectrum is shown in Figure 4b.

**Table VI**
**Tetrad (PR-Tetrad) Tacticity in the Chain-End Structure I**

| tetrad in the chain end | I obsd | inner chain | |
|---|---|---|---|
| | | tetrad | obsd |
| PR-*mmm* | 0.482 | *mmm* | 0.546 |
| PR-*mmr* | 0.055 | *mmr* | 0.158 |
| PR-*rmm* | 0.128 | | |
| PR-*rmr* | 0.063 | rmr | 0.032 |
| PR-*mrm* | 0.030 | mrm | 0.046 |
| PR-*mrr* | 0.085 | mrr | 0.135 |
| PR-*rrm* | 0.066 | | |
| PR-*rrr* | 0.092 | rrr | 0.084 |

as yet. The fractions of chain-end tetrads are determined from the relative areas of the peaks by using the curve resolution method[19] and the results for PPS7 are shown in Table VI. The inner-chain tetrad tacticity determined from the relative peak areas of the methylene resonances based on the hexad assignments proposed by Schilling and Tonelli[14] is also shown in Table IV for a comparison. The respective tetrad fractions of the chain-end region are similar to those of the inner-chain region except the PR-*rmr* and -*rmr* tetrads.

In parts a and b of Figure 5 are shown the spectral region of 29.5–31.5 ppm of PP and PPS7, respectively. A $^1$H-decoupled INEPT spectrum ($\Delta = 3/4J$) of PPS7 is shown in Figure 5c, in which only one methylene peak is appeared at 30.01 ppm. The corresponding peak is not observed in the spectrum of PP. Referring to the chemical shifts of carbon 7-(B) shown in Table I, the peak at 30.01 ppm is assigned to methylene carbon 2 (2-(II)) in structure II of ET-meso, because that shift agrees well with that of carbon 7-(B) of meso form (29.95 ppm). Further, the intensity of the peak at 30.01 ppm is as strong as that at 11.12 ppm as shown in Figure 2a. The peak of carbon 2-(II) of ET-racemo is undetected in the spectrum of PPS7, while the split peaks of carbon 2-(II) at 29.75 and 30.85 ppm, which should arise from the different diad configurations around methylene carbon 4, were observed in the spectrum of polypropylene prepared with the $\delta$-$TiCl_3$–Al-($^{13}CH_2CH_3$)$_3$–Zn($^{13}CH_2CH_3$)$_2$ catalytic system.[4]

The peak observed at 30.65 ppm in the spectra of both PP and PPS7 is assigned to carbon 4 (4-(I)) in structure I, since its chemical-shift value corresponds to that of carbon 6-(A) and the intensity of the peak at 30.65 ppm

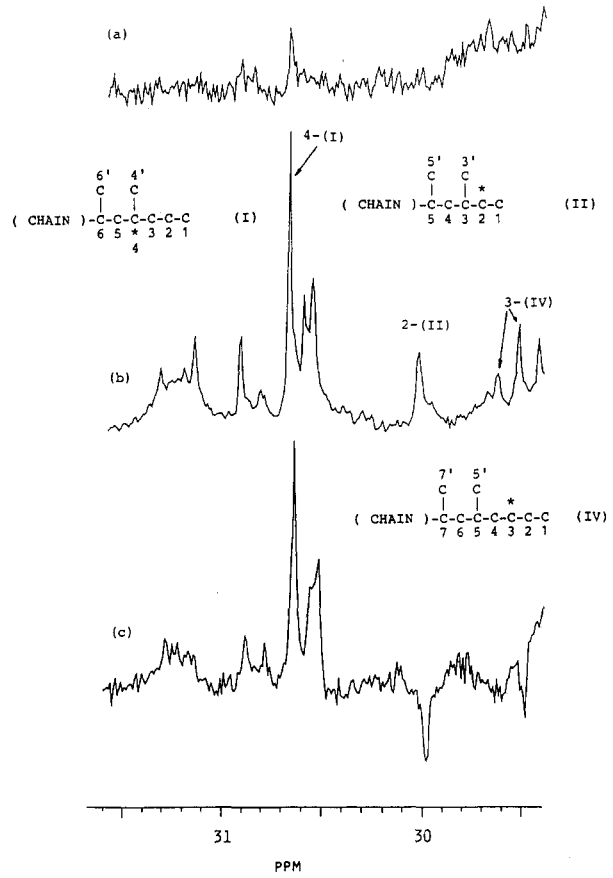


**Figure 5.** Regions from 29.5 to 31.5 ppm in the $^{13}$C NMR spectra of (a) PP and (b) PPS7. (c) $^1$H-decoupled INEPT ($\Delta = 3/4J$) spectrum of PPS7.

is nearly equal to that at 14.49 ppm. The chemical shift difference between the peaks at 30.65 and 30.58 ppm and that between the peaks at 30.65 and 30.53 ppm are 0.07 and 0.12 ppm, respectively. Since the chemical shift difference in carbon 6-(A) due to the configurational difference in structure A is only 0.04 ppm as shown in Table I, the observed chemical shift differences are too large to assign the peaks at 30.53 and 30.58 ppm to carbon 4-(I). Thus, the peaks at 30.53 and 30.58 ppm are unidentified. From these results, it is confirmed that structure I exists in both PPS7 and PP, while structure II only in PPS7.

In parts a and b of Figure 6 are shown the region of 22.5–24 ppm. Only two peaks are observed for PP, while a number of split peaks are observed for PPS7. Referring to the chemical shifts of carbons 1 and 2′ in both compounds A and B shown in Table I, the split peaks are assigned to the carbons 1 and 2′ in chain-end structure III.

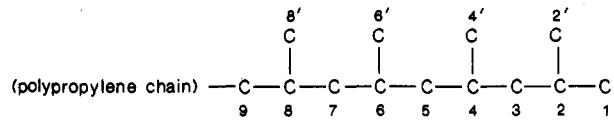


III

The chemical shifts due to the $\gamma$-effect was calculated for the carbons 1 and 2′ in structure III with the tactic triads (ME-triads), which are determined by the configurational relationships among the methine carbons 4, 6, and 8. Again, the polypropylene chain is simplified to be a chain composed of 20 meso diads except the sequences including methine carbons 4, 6, and 8. The calculated chemical shift differences of carbons 1 and 2′ in structure III are shown in the Table VII with the observed chemical shifts of PPS7. The peaks appearing at 22.58 and 23.82 ppm are assigned to carbons 1 and 2′ in structure III with

**Table VII**
**Calculated and Observed Chemical Shift Differences ($\Delta\nu$) of Carbons 1 and 2′ in Chain-End Structure III**

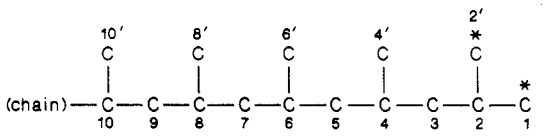


III

| triad in the chain end | carbon 1 | | | | carbon 2′ | | | |
|---|---|---|---|---|---|---|---|---|
| | calcd γ-effect, ppm | $\Delta\nu_{calcd}$,[a] ppm | $\nu_{obsd}$,[b] ppm | $\Delta\nu_{obsd}$,[a,b] ppm | calcd γ-effect, ppm | $\Delta\nu_{calcd}$,[a] ppm | $\nu_{obsd}$,[b] ppm | $\Delta\nu_{obsd}$,[a,b] ppm |
| ME-*mm* | −1.852 | 0.0 | 23.82 | 0.0 | −3.637 | 0.0 | 22.58 | 0.0 |
| ME-*mr* | −2.036 | −0.138 | 23.75 | −0.07 | −3.453 | 0.184 | 22.65 | 0.07 |
| ME-*rr* | −2.248 | −0.396 | 23.54 | −0.28 | −3.241 | 0.396 | 22.82 | 0.24 |
| ME-*rm* | −2.389 | −0.537 | 23.49 | −0.33 | −3.100 | 0.537 | 22.87 | 0.29 |

[a] Chemical shifts are expressed relative to the peak appearing at the lowest field which is set to be 0.00 ppm. [b] Chemical shifts $\nu$ and chemical shift differences $\Delta\nu$ observed for PPS7. Corresponding spectrum is shown in Figure 6b.

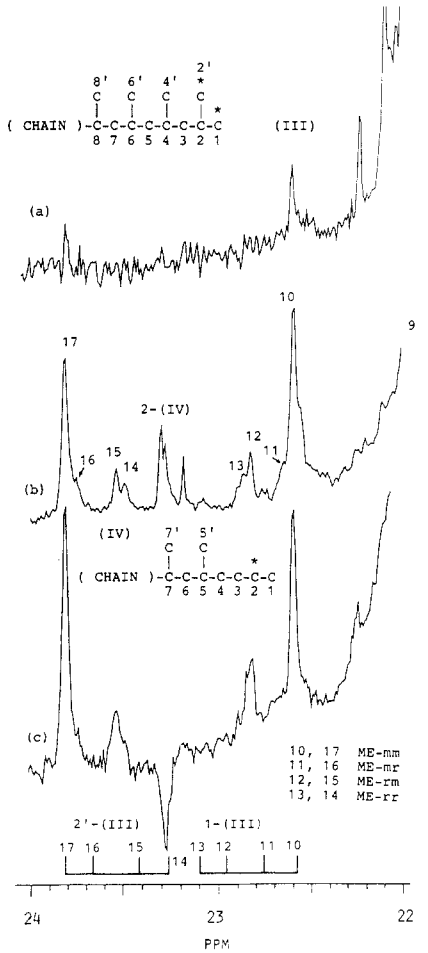


**Figure 6.** Regions from 22.5 to 24.0 ppm in the $^{13}C$ NMR spectra of (a) PP and (b) PPS7. (c) $^{1}H$-decoupled INEPT ($\Delta = 3/4J$) spectrum of PPS7. The predicted shifts are shown as the stick spectrum at the bottom of this figure.

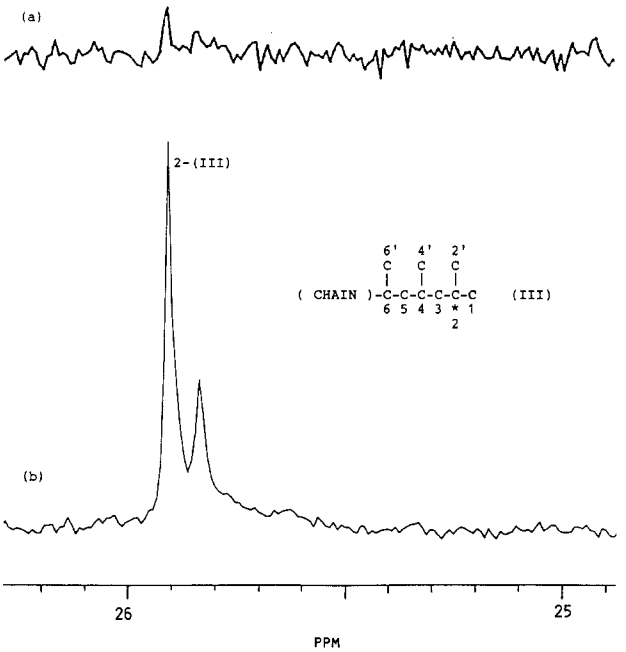


**Figure 7.** $^{13}C$ NMR spectra of methine carbon 2 in the chain-end structure III of (a) PP and (b) PPS7.

**Table VIII**
**Assignments and Relative Areas of the Peaks Attributable to the Methyl Carbons 1 and 2′ in the Chain-End Structure III**

| peak | obsd, ppm | triad in the chain end ME- | rel peak area |
|---|---|---|---|
| 10 | 22.58 | *mm* | 0.042 |
| 11 | 22.65 | *mr* | 0.009 |
| 12 | 22.82 | *rr* | 0.014 |
| 13 | 22.87 | *rm* | 0.007 |
| 14 | 23.49 | *rm* | 0.008 |
| 15 | 23.54 | *rr* | 0.011 |
| 16 | 23.75 | *mr* | 0.008 |
| 17 | 23.82 | *mm* | 0.035 |
| 9[a] | 21.86 | | 1.000 |

[a] Assigned to be *mmmm* pentad.

an ME-*mm* configuration, because the calculation via the γ-effect predicts that the peaks of carbons 1 and 2′ of ME-*mm* should appear at the lowest and the highest field, respectively. The predicted chemical shifts are illustrated as a stick spectrum in Figure 6. By comparison between the observed and calculated spectra, the assignments of the split peaks numbered 10–16 are provided as shown in Table VIII. The assignments of the peaks observed at 23.28 and 23.30 ppm will be described later. Further, the relative areas of peaks 10, 11, 12, and 13 are nearly equal to those of peaks 17, 16, 15, and 14, respectively. This also assures our assignments of these peaks.

As shown in Figure 7, two peaks are observed at 25.83 and 25.91 ppm in the spectrum of PPS7 as shown in Figure 7b, while a very small peak is observed only at 25.91 ppm for PP. These peaks are assigned to carbon 2 in structure III, because these chemical shifts agree with the that of carbon 2 in the compound A. Further, the chemical-shift

**Table IX**
**Chemical Shifts of the Carbons 1–5 in the Chain-End Structure IV**

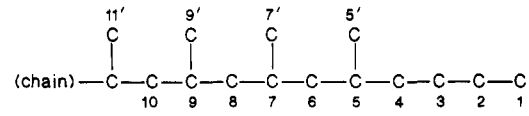


IV

| carbon | predicted,[a] ppm | predicted,[b] ppm | obsd, ppm |
|---|---|---|---|
| 1 | 14.05 | 14.1 | 14.12 |
| 2 | 22.90 | 23.0, 23.1 | 23.28, 23.30 |
| 3 | 29.71 | 29.3, 29.4 | 29.51, 29.61 |
| 4 | 36.91 | 37.4, 38.2 | 37.06, 37.30, 37.94 |
| 5 | 30.39 | 31.1, 31.1 | 30.89 or 31.13 |

[a] Predicted by Linedeman–Adams' empirical rule.[20] [b] Predicted by Cheng et al.[6]

differences in carbon 2 in compound A due to the change of chain-end diads (ME-diads) is predicted to be 0.045 ppm (the chemical shift of the carbon 2 in A of ME-meso is predicted to be 0.045 ppm larger than that of ME-racemo). This value corresponds to the chemical shift difference of 0.072 ppm observed in the spectrum. Thus, the peaks at 25.905 and 25.833 ppm are assigned to the methine carbon 2 in the chain-end structure (III) of ME-meso and ME-racemo, respectively.

The existence of chain-end structure IV in PPS7 is

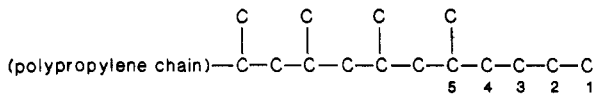


IV

confirmed from its $^{13}C$ NMR spectrum. In Table IX are shown the chemical shifts of the carbons 1–5 in structure IV, which are predicted by Cheng et al.[6] and by us using Linedeman–Adams' empirical rule[20] and the corresponding chemical shifts observed in the spectrum. These peaks are undetected in the spectrum of PP. By comparison among the observed and predicted chemical shifts, the peaks attributable to carbons 1–5 are assigned as follows: The peak at 14.05 ppm in Figure 1b is assigned to carbon 1 (1-(IV)) with good agreement among the predicted and observed chemical shifts. The peaks at 23.28 and 23.30 ppm in Figure 6b are assigned to methylene carbons 2 (2-(IV)) on the basis of the INEPT ($\Delta = 3/4J$) spectrum shown in Figure 6c and the prediction by Cheng et al.[6] The peak at 23.18 ppm was unidentified. The peaks at 29.51 and 29.61 ppm in Figure 5b are assigned to methylene carbons 3 from the INEPT spectrum shown in Figure 5c and the chemical shifts predicted by us using Lindeman–Adams' empirical rule and by Cheng et al. The peaks at 30.89 and 31.13 ppm in Figure 5b would be assigned to the carbon 5. The peaks at 37.06, 37.30, and 37.94 ppm in Figure 8 are assigned to methylene carbon 4 by comparison with the chemical shifts predicted by Cheng. The peak at 36.61 ppm was unidentified, though the INEPT spectrum indicates that this is the resonance of the methine carbon. In Table X are shown the calculated and observed chemical shift differences in carbons 2–4 due to the difference in chain-end diad or triad configurations. The respective chemical shift differences in carbons 2 and 3 predicted by the calculation via the $\gamma$-effect agree well with observed ones, indicating the validity of our assignments. The chemical shift differences in the resonance of carbon 4 due to the difference in chain-end triad configuration are predicted by the $\gamma$-effect calculation and the results are illustrated in Figure 8 as a stick spectrum. By the

**Table X**
**Chemical Shifts ($\nu$) of the Peaks Attributable to the Carbons 2–4 in the Chain-End Structure IV**

| carbon | $n$-ad in the chain end BU-diad and BU-triad | calcd $\gamma$-effect, ppm | $\Delta\nu_{calcd}$,[a] ppm | $\nu_{obsd}$, ppm | $\Delta\nu_{obsd}$,[a] ppm |
|---|---|---|---|---|---|
| 2 | *m* | −0.927 | 0.028 | 23.30 | 0.02 |
| 2 | *r* | −0.955 | 0.0 | 23.28 | 0.0 |
| 3 | *m* | −4.486 | 0.0 | 29.51 | 0.0 |
| 3 | *r* | −4.369 | 0.117 | 29.61 | 0.10 |
| 4 | *mm* | −3.897 | 0.0 | 37.06 | 0.0 |
| 4 | *mr* | −3.495 | 0.402 | 37.30 | 0.24 |
| 4 | *rm* | −2.699 | 1.198 | 37.94 | 0.88 |
| 4 | *rr* | −3.020 | 0.877 | | |

[a] Chemical shifts are expressed relative to the peak appearing at the highest field which is set to be 0.00 ppm.

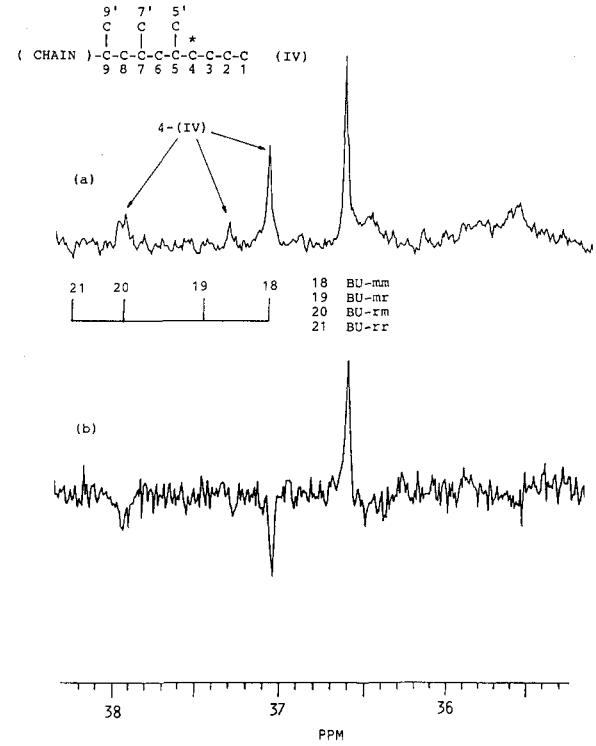


**Figure 8.** (a) $^{13}C$ NMR spectra of methylene carbon 4 in the chain-end structure IV of PPS7. (b) $^{1}H$-decoupled INEPT ($\Delta = 3/4J$) spectrum of PPS7.

comparison between the observed and calculated spectra, the peaks at 37.06 and 37.3 ppm are assigned to carbons 4 (4-(IV)) in structure IV with BU-*mm* and BU-*mr* configurations, respectively. The peak at 37.94 ppm is assigned to carbon 4-(IV) of BU-*rm* or BU-*rr*.

**Schemes for the Formation of Chain-End Structures.** From the $^{13}C$ NMR analyses of chain-end structures, the existence of structures I–IV in PPS7 and those of I and III in PP are confirmed. Referring to the studies on the chain-end structures by Zambelli et al.,[2,4] structure II is produced by the primary insertion of the propylene monomer on a metal (M)–$CH_2CH_3$ bond in the initiation step. The scheme is

$$M{-}CH_2CH_3 + CH_2{=}CHCH_3 \xrightarrow{\text{primary insertion}}$$
$$M{-}CH_2CH(CH_3)CH_2CH_3 + CH_2{=}CHCH_3 \xrightarrow{\text{propagation}}$$
II (1)

where the ethyl group of M–$CH_2CH_3$ is derived from

$Et_2AlCl$ used as an organometallic compound.

As shown in the INEPT spectrum of Figure 5c, a single peak of methylene carbon 2-(II) of ET-meso is observed in the spectrum of PPS7, and also observed is a single peak of carbon 1-(II) in Figure 2b. This indicates that in the polymerization with a $\delta$-$TiCl_3/Et_2AlCl$ catalytic system the strong stereospecific control on adding monomer operates even at the initiation reaction.

A possible scheme for the production of structure IV is the termination reaction of the propagating species M–(chain) by hydrogen when the propylene inserts through secondary insertion as follows:

$$\begin{aligned} &M\text{—(chain)} + CH_3CH{=}CH_2 \xrightarrow{\text{secondary insertion}} \\ &\quad M\text{—}CH(CH_3)CH_2CH_2CH(CH_3)\text{—(chain)} + \\ &\quad H_2 \xrightarrow{\text{termination}} \\ &M\text{—H} + CH_3CH_2CH_2CH_2CH(CH_3)\text{—(chain)} \quad \text{IV} \quad (2) \end{aligned}$$

An another possible scheme for the formation of identified structure IV is the copolymerization with ethylene at the initiation reaction and the subsequent primary insertions of propylene as follows:

$$\begin{aligned} &M\text{—}CH_2CH_3 + CH_2{=}CH_2 \xrightarrow{\text{ethylene insertion}} \\ &\quad M\text{—}(CH_2)_3CH_3 \xrightarrow{\text{propylene insertion}} \\ &M\text{—}CH_2CH(CH_3)(CH_2)_3CH_3 \xrightarrow{\text{further propylene insertion}} \text{IV} \quad (3) \end{aligned}$$

The source of the ethylene was ascribed to the impurity included in the propylene monomer and the decomposition reactions of $Cl_2Ti$–Et.[21-25] However, since the peak assigned undoubtedly to $S_{\alpha\gamma}$ carbon, which arises from the isolated ethylene unit in the polypropylene chain, is not observed in Figure 8 on the basis of the assignments by Ray et al.[26] (where the chemical shift of the carbon $S_{\alpha\gamma}$ is 37.8 ppm), the contribution of this scheme for the production of the structure IV is negligible.

On the basis of the chain-end structures,[2-4] it is reasonable to conclude that propylene polymerizes mainly through primary insertion, since $\delta$-$TiCl_3$ is a stereoregular type catalyst. Thus, the possible scheme for the formation of structure I is the primary insertion of propylene on the metal (M)–H bond[21,22] and the subsequent primary insertions of propylene monomers. Another possible scheme is the chain-transfer reaction of the propagation species to the propylene monomer[21,22] and the subsequent primary insertions of propylene. In our polypropylene sample, structure I should be mainly produced through the former scheme, because hydrogen is effective for lowering the molecular weight of resulting polypropylene.[21,22] The scheme of the termination reaction by hydrogen[12] is

$$M\text{—(chain)} + H_2 \xrightarrow{\text{termination}} M\text{—H} + \text{(chain)—H} \quad (4)$$

Structure III is formed via the same reaction by the primary insertion of propylene as follows:

$$\begin{aligned} &M\text{—}CH_2CH(CH_3)CH_2\text{—(chain)} \xrightarrow{\text{termination by } H_2} \\ &\quad M\text{—H} + CH_3CH(CH_3)CH_2\text{—(chain)} \quad \text{III} \quad (5) \end{aligned}$$

The active center is regenerated when propylene monomer adds to the M–H bond.

$$\begin{aligned} &M\text{—H} + CH_2{=}CHCH_3 \xrightarrow{\text{insertion}} \\ &\quad M\text{—}(CH_2)_2CH_3 \xrightarrow{\text{further propylene insertion}} \\ &M\text{—}CH_2CH(CH_3)(CH_2)_2CH_3 \xrightarrow{\text{propagation}} \text{I} \quad (6) \end{aligned}$$

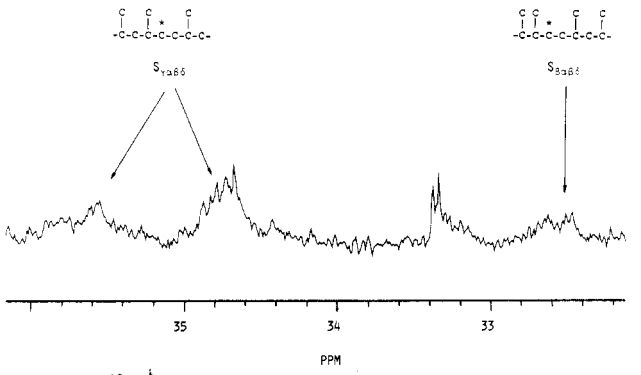


**Figure 9.** $^{13}C$ NMR spectrum of the $S_{\beta\alpha\beta\delta}$ and $S_{\gamma\alpha\beta\delta}$ carbons of PPS7.

**Table XI**
**Mole Fractions of the Chain-End Structures I, II, III, and IV Determined from the Relative Areas of the Peaks of the Methyl Carbons 1 in these Structures**

| | structure | | | |
|---|---|---|---|---|
| | I | II | III | IV |
| mole fractn | 0.459 | 0.041 | 0.401 | 0.099 |

The scheme for the chain-transfer reaction of the propagation species to the propylene monomer is

$$\begin{aligned} &M\text{—(chain)} + CH_2{=}CHCH_3 \xrightarrow{\text{chain transfer and } H_2 \text{ addition}} \\ &\quad M\text{—}CH_2CH_2CH_3 + \text{(chain)—H} \end{aligned}$$

$$\begin{aligned} &M\text{—}CH_2CH_2CH_3 + CH_2{=}CHCH_3 \rightarrow \\ &\quad M\text{—}CH_2CH(CH_3)CH_2CH_2CH_3 \xrightarrow{\text{propagation}} \text{I} \quad (7) \end{aligned}$$

In Table XI are shown the mole fractions of the chain-end structures I–IV determined from the relative areas of the peaks of carbon 1 in these structures. Apparently, structures I and II are formed through the initiation reactions (1), (6), and (7) and the subsequent propagation reactions and structures III and IV through the termination reactions (4) and (2). The sum of the mole fractions of structures I and II is 0.5, which is equal to the sum of those of structures III and IV. The equality of these two values assures the schemes for the formation of chain-end structures. As shown in Figure 9, the peaks attributable to $S_{\beta\alpha\beta\delta}$ and $S_{\gamma\alpha\beta\delta}$ carbons in the regioirregular polypropylene[27,28] are observed in the spectrum of PPS7, where the designations $S_{\beta\alpha\beta\delta}$ and $S_{\gamma\alpha\beta\delta}$ are based on the terminology of Cheng.[27] The intensities of these peaks are too small for quantitative analysis. The $S_{\beta\alpha\beta\delta}$ and $S_{\gamma\alpha\beta\delta}$ peaks are not detected in the spectrum of PP, indicating that the subsequent propagation reaction is unlikely to occur even if the secondary insertion of propylene occurs. From the ratio of the peak area of the methyl groups in the chain and that of the methyl carbons 1 in structures I and II, the number-average molecular weight of PPS7 is determined to be 1220, which agrees well with that of 1000 determined by gel permeation chromatography.

In the spectrum of PP, carbon 3-(I) shows a single peak corresponding to PR-*mmm* and carbons 1-(III) and 2′-(III) show two peaks corresponding to ME-*mm*. Thus, only the isotactic sequences are found in the chain-end structures of PP. This indicates that in the whole polymer the isotactic control for the primary insertion of propylene on the M–H bond is as strong as that on the M–(chain) bond, because the observed chain-end *n*-ads are as highly isotactic as those in the chain. The disappearance of structure II in the whole polymer suggests that the initiation reaction of the most parts of the propylene polymerization proceeds by a primary insertion of propylene on the M–H bond.

**Table XII**
**Triad Tacticities in the Chain-End Structures I and III**

| *n*-ad in the chain end | obsd I PR-triad and -diad | obsd III ME-triad and -diad | *n*-ad inner chain triad and diad | obsd |
|---|---|---|---|---|
| *mm* | 0.579 | 0.537 | *mm* | 0.521 |
| *mr* | 0.121 | 0.115 | *mr* | 0.232 |
| *rm* | 0.111 | 0.191 | | |
| *rr* | 0.189 | 0.158 | *rr* | 0.247 |
| *m* | 0.700 | 0.652 | *m* | 0.637 |
| *r* | 0.300 | 0.349 | *r* | 0.363 |

**Table XIII**
**Determined Values of the Three Parameters for the Two-Site Model**

| sample | $\omega$ | $\alpha$ | $\sigma$ |
|---|---|---|---|
| PP | 0.938 | 0.990 | 0.351 |
| PPS7 chain | 0.669 | 0.908 | 0.232 |
| PPS7 I | 0.550 | 0.979 | 0.312 |
| PPS7 III | 0.540 | 0.924 | 0.479 |

In the case of PPS7, the ratio of structure I/structure II is approximately 11.3, as shown in Table XI, indicating that the main initiation reaction is a primary insertion of propylene on the M–H bond which is formed by the termination reaction with molecular hydrogen.

Further, in Table XII are shown the triad tacticities at the chain end of structures I and III. The chain-end triads in structure I were estimated from the values of the chain-end tetrads by using the triads–tetrads relationships. The triads in the chain were determined in a previous paper.[11] The fractions of diads were obtained from the triads–diads relationships. The fractions of each triad and diad at the chain end are comparable to those in the inner chain. According to our preceding results,[11] the propagation mechanism of propylene is reasonably described by using the two-site model, in which polymerization at one site (symmetric site) proceeds according to the Bernoullian model of selection between meso (*m*) and racemo (*r*) configurations, while at the other site (asymmetric site) proceeds according to selection between dextro (*d*) and levo (*l*). The two-site model permits a description of the triad and pentad tacticities reasonably with three parameters: $\alpha$, the probability of selecting a d-unit at a d-preferring site in the asymmetric site; $\sigma$, the probability of selecting a meso diad configuration in the symmetric site; and $\omega$, the weight fraction of the polymer produced at the asymmetric site. In Table XIII are shown the estimated values of three parameters of the two-site model. The values of triad tacticity for PP and PPS7 are reproduced quite well by the two-site model using these parameters within standard deviations of less than 0.0005. The results of two-site model analysis indicate that both PP and PPS7 are composed of two kinds of polymer chains or sequences: one is highly isotactic, produced at the asymmetric site, while the other is atactic, produced at the symmetric site. Thus, the observed split peaks due to chain-end tetrads or triads in the spectrum of PPS7 arise mainly from the atactic polypropylene with weight fraction of 0.331, which is produced at the symmetric site, because the contribution from the isotactic polypropylene produced at asymmetric site is rather small owing to the large $\alpha$ value of 0.908. The tacticity of polypropylene produced at the symmetric site is atactic at both the chain end and the inner chain. As for the whole polymer, only isotactic sequences are detected in the chain-end structures and the weight fraction, $\omega$, of the polymer produced at the asymmetric site is 0.938. The tacticity of polypropylene produced at the asymmetric site is isotactic at both the chain end and the inner chain. Therefore, the respective steric controls of the initiation reactions at the symmetric and asymmetric sites are as strong as those of atactic and isotactic propagation reactions, respectively.

## Conclusions

Four chain-end structures of polypropylene polymerized with a $\delta$-$TiCl_3/Et_2AlCl$ catalytic system in the presence of hydrogen are identified on the basis of $^1H$-decoupled $^{13}C$ NMR and INEPT spectra. The chain-end structures I and II are produced with the initiation reactions and the subsequent propagation reactions. The chain-end structures III and IV are produced by the termination reactions. Further, high-resolution $^{13}C$ NMR spectra enable us to analyze the tacticity of the triad and tetrad sequence in the chain end. The assignments of the split peaks of the carbons in the end groups due to the different stereosequences in the chain-end structures are provided by the chemical shifts calculation via the $\gamma$-effect. In particular, the chain-end tetrads in structure I, which is produced with the initiation reaction by the primary insertion of propylene on a metal–hydrogen bond and the subsequent propagation reaction, are determined. The tacticity in chain-end structure I reflects the steric control of the catalyst at the initiation reaction in the presence of hydrogen, because a metal–hydrogen bond is produced by the termination reaction with hydrogen. By use of the two-site model for the polymerization process, it is concluded that the respective steric controls of the initiation reaction at the asymmetric and symmetric sites are as strong as those of isotactic and atactic propagation reactions, respectively.

**Acknowledgment.** We thank Associate Professor Yoshiharu Doi at Research Laboratory of Resources Utilization, Tokyo Institute of Technology, for helpful discussions concerning the schemes for the formation of chain-end structures. We thank Mr. Hidetoshi Kawamura at Polymer Development Laboratory, Tokuyama Soda Co. Ltd., for the measurement of the $^{13}C$ NMR spectra. T.H. expresses his sincere thanks to Tokuyama Soda Co. Ltd. for leave from the company to develop this study at Tokyo Institute of Technology.

**Registry No.** PP, 9003-07-0; $TiCl_3$, 7705-07-9; $Et_2AlCl$, 96-10-6; propylene, 115-07-1; hydrogen, 1333-74-0.

## References and Notes

(1) Zambelli, A.; Locatelli, P.; Bajo, G. *Macromolecules* **1979**, *12*, 154.
(2) Zambelli, A.; Locatelli, P.; Rigamonti, E. *Macromolecules* **1979**, *12*, 156.
(3) Zambelli, A.; Locatelli, P.; Sacchi, M. C.; Rigamonti, E. *Macromolecules* **1980**, *13*, 798.
(4) Zambelli, A.; Sacchi, M. C.; Locatelli, P.; Zannoni, E. *Macromolecules* **1982**, *15*, 211.
(5) Ammendola, P.; Vitagliano, A.; Oliva, L.; Zambelli, A. *Makromol. Chem.* **1984**, *185*, 2421.
(6) Cheng, H. N.; Smith, D. A. *Macromolecules* **1986**, *19*, 2065.
(7) Chûjô, R. *Kagaku* **1980**, *13*, 267.
(8) Zambelli, A.; Locatelli, P.; Provasoli, A.; Fero, D. R. *Macromolecules* **1980**, *13*, 267.
(9) Zhu, S. N.; Yang, X. Z.; Chûjô, R. *Polym. J.* **1983**, *15*, 859.
(10) Inoue, Y.; Itabashi, Y.; Chûjô, R.; Doi, Y. *Polymer* **1984**, *25*, 1640.
(11) Hayashi, T.; Inoue, Y.; Chûjô, R.; Asakura, T. *Polymer* **1988**, *29*, 138.
(12) Natta, G. *Chim. Ind. (Milan)* **1959**, *41*, 519.
(13) Tonelli, A. E. *Macromolecules* **1978**, *11*, 565.
(14) Schilling, F. C.; Tonelli, A. E. *Macromolecules* **1980**, *13*, 270.
(15) Mark, J. E. *J. Chem. Phys.* **1972**, *57*, 2541.
(16) Burum, D. P.; Ernst, R. R. *J. Magn. Reson.* **1980**, *39*, 163.
(17) Doddrell, D. M.; Pegg, D. T. *J. Am. Chem. Soc.* **1980**, *102*, 6388.
(18) Tonelli, A. E. *Macromolecules* **1979**, *12*, 255.

(19) Randall, J. C. *J. Polym. Sci., Polym. Phys. Ed.* **1976**, *14*, 2083.
(20) Lindeman, L. P.; Adams, J. Q. *Anal. Chem.* **1971**, *43*, 1245.
(21) Kissin, Y. V. *Isospecific Polymerization of Olefins*; Springer-Verlag: New York, 1985.
(22) Boor, J., Jr. *Zieglar–Natta Catalysts and Polymerizations*; Academic: New York, 1979.
(23) Atarashi, Y. *Chem. High Polym. (Jpn.)* **1964**, *21*, 257.
(24) Atarashi, Y. *Chem. High Polym. (Jpn.)* **1964**, *21*, 409.
(25) Burfield, D. R. *J. Polym. Sci., Polym. Chem. Ed.* **1978**, *16*, 3301.
(26) Ray, G. J.; Johnson, P. E.; Knox, J. R. *Macromolecules* **1977**, *10*, 773.
(27) Cheng, H. N. *Polym. Bull. (Berlin)* **1985**, *14*, 347.
(28) Asakura, T.; Nishiyama, Y. *Macromolecules* **1987**, *20*, 616.

# Comblike Polysiloxanes with Oligo(oxyethylene) Side Chains. Synthesis and Properties

**Ishrat M. Khan, Youxin Yuan, Daryle Fish, E Wu, and Johannes Smid***

*Polymer Research Institute, Chemistry Department, College of Environmental Science and Forestry, State University of New York, Syracuse, New York 13210.*
*Received November 24, 1987*

ABSTRACT: Comb polysiloxanes with oligo(oxyethylene) side chains of the type $-O(CH_2CH_2O)_nCH_3$ were synthesized from poly(methylsiloxane) and zinc octanoate as catalyst. The comb polymers, abbreviated as PMMS (followed by a number indicating the number of oxygen atoms in the side chain), were characterized by FTIR, NMR ($^1H$ and $^{29}Si$), and GPC. Thermal properties were studied by DSC. A considerable fraction of cyclics was found to be present in the polymers, and redistribution reactions result in comb polymers containing branched trisiloxy units. Side-chain crystallization is observed in all polymers except PMMS-5. Polymers with 5, 12, 16, and 22 oxygen atoms in the side chain are water-insoluble, but PMMS-8 was soluble enough to carry out cloud-point measurements in the presence of salts.

## Introduction

We recently reported on the conductivity of solid complexes of lithium perchlorate with poly{[ω-methoxyhexakis(oxyethylene)ethoxy]methylsiloxane}, a comblike polysiloxane with pendant oligo(oxyethylene) groups containing an average of seven oxyethylene units.[1,2] Conductivities of $7 \times 10^{-5}\ \Omega^{-1}\ cm^{-1}$ at 25 °C and between $10^{-4}$ and $10^{-3}\ \Omega^{-1}\ cm^{-1}$ at higher temperatures were found depending on the salt content of the polymer and the degree of cross-linking. While the importance of siloxane–oxyethylene block and graft copolymers has been known since the 1950s,[3] it is only recently that polysiloxane comb polymers with oligo(oxyethylene) side chains have been synthesized. Bannister et al.[4,5] synthesized such comb polymers because of their potential application in cryobiology while the conducting properties of their salt complexes were also investigated.[6] The polymers can be synthesized from poly(methylsiloxane) (PHMS) and a methoxypoly(ethylene glycol) (MPEG) with the aid of a basic catalyst. The reaction results in the elimination of hydrogen gas and the formation of the $Si–O(CH_2CH_2O)_nCH_3$ group. Kohama et al. have investigated a number of catalysts for the reaction of low molecular weight alcohols with PHMS.[7] Bannister used 2 mol of triethylamine/mol of Si–H and a reaction time of approximately 30 days. Our synthesis was carried out in THF with zinc octanoate as catalyst (*about 0.2% of available Si–H groups*) and a reaction time of 48 h to 1 week depending on the length of the MPEG. Metal octanoate catalysts have previously been employed in the preparation of model elastomeric polysiloxane networks.[8]

Because of their potential application in areas such as solid polymer electrolytes, foam stabilizers,[3] and biocompatible materials,[4,9] it is desirable to have definitive structural assignments for the comb polymers and to address the problem of chemical redistribution, an inherent property of polysiloxanes. In this paper the details of the synthesis and characterization of poly{[ω-methoxyoligo(oxyethylene)ethoxy]methylsiloxane}s by $^1H$ and $^{29}Si$ NMR, FTIR, elemental analysis, and GPC studies are reported.

## Experimental Section

**Materials.** Poly(methylsiloxane) (PHMS), zinc octanoate (in poly(dimethylsiloxane)), and 1,3,5,7-tetramethylcyclotetrasiloxane (D4H) were purchased from Petrarch. The number average molecular weight of PHMS was determined by 100-MHz $^1H$ NMR by comparing the trimethylsiloxy end groups with the internal methyl group. Its value was found to be 2650. Methoxypoly(ethylene glycol)s (MPEG) of molecular weight 250, 350, 550, and 750 were Sigma products. MPEG-1000 was obtained by hydrolysis of methoxypoly(ethylene glycol) monomethacrylate (Polysciences) with a reported MPEG ester group of 1000. The hydrolysis was carried out in 0.1 N NaOH at 25 °C for 16 h. The MPEG-1000 was extracted into chloroform, the extract washed with water and dried, and the solvent removed. The final product and MPEG-750 were freeze-dried from benzene, while MPEG 250, 350, and 550 were dried by repeated azeotropic distillation with benzene on a rotary evaporator at reduced pressure.

**Synthesis.** Poly{[ω-methoxyoligo(oxyethylene)ethoxy]methylsiloxane}s, abbreviated as PMMS-*n*, were synthesized by adding a slight excess of the appropriate MPEG compound to a THF solution of PHMS (1 g/50 mL) and zinc octanoate as catalyst (*about 0.002 mol/mol of Si–H groups*). The temperature was kept at 60 °C, and the reaction times were 48 h for MPEG-250 and MPEG-350, 72 h for MPEG-550, and 7 days for MPEG-750 and MPEG-1000. After removal of solvent the polymers were purified by repeated precipitation into a 90/10 (v/v) mixture of hexane and THF to remove unreacted MPEG. The purity of the polymers was checked by 100-MHz $^1H$ NMR, $^{29}Si$ NMR, IR, GPC, and elemental analysis. The five polymers have been abbreviated as PMMS-5, -8, -12, -16, and -22, the number referring to the average number of oxygen atoms in the oligo(oxyethylene) side chain of the comb polymer.

The model cyclic tetramer 1,3,5,7-tetrakis[ω-methoxyhexakis(oxyethylene)ethoxy]-1,3,5,7-tetramethylcyclotetrasiloxane or D4G-8 was made from D4H and MPEG-350 in THF under conditions similar to those outlined for the corresponding polymer

0024-9297/88/2221-2684$01.50/0 